0026-895X/03/6404-954–964$7.00
MOLECULAR PHARMACOLOGY
Vol. 64, No. 4
2523/1092601
Mol Pharmacol 64:954–964, 2003
Printed in U.S.A.

Contrasting Actions of Philanthotoxin-343 and Philanthotoxin-(12) on Human Muscle Nicotinic Acetylcholine Receptors

TIM J. BRIER, IAN R. MELLOR, DENIS B. TIKHONOV, IOANA NEAGOE, ZUOYI SHAO, MATT J. BRIERLEY, KRISTIAN STRØMGAARD, JERZY W. JAROSZEWSKI, POVL KROGSGAARD-LARSEN, AND PETER N. R. USHERWOOD

Division of Molecular Toxicology, School of Life and Environmental Sciences, University of Nottingham, Nottingham, United Kingdom (T.J.B., I.R.M., I.N., Z.S., M.J.B. and P.N.R.U.); Department of Medicinal Chemistry, The Danish University of Pharmaceutical Sciences, Copenhagen, Denmark (K.S., J.W.J. and P.K-L.); and Sechenov Institute of Evolutionary Physiology and Biochemistry, Russian Academy of Sciences, St. Petersburg, Russia (D.B.T.).

Received March 13, 2003; accepted June 18, 2003

This article is available online at http://molpharm.aspetjournals.org

ABSTRACT

Whole-cell recordings and outside-out patch recordings from TE671 cells were made to investigate antagonism of human muscle nicotinic acetylcholine receptors (nAChR) by the philanthotoxins, PhTX-343 and PhTX-(12). When coapplied with acetylcholine (ACh), PhTX-343 caused activation-dependent, noncompetitive inhibition (IC_{50} = 17 μM at −100 mV) of whole-cell currents that was strongly voltage-dependent. However, preapplication of PhTX-343 unveiled a voltage-independent antagonism that also required receptor activation, which is suggestive of desensitization enhancement. In single-channel studies, 10 μM PhTX-343 significantly reduced the mean open time of channel openings evoked by 1 μM ACh from 4.42 ± 0.44 to 1.58 ± 0.10 ms with a minor increase (1.26-fold) in mean closed time. These data indicate that PhTX-343 predominantly blocks the open channel gated by ACh. In contrast, PhTX-(12) caused potent (IC_{50} = 0.77 μM at −100 mV), activation-dependent, noncompetitive inhibition of ACh-induced whole-cell currents that was only weakly voltage-dependent and suggestive of desensitization enhancement. It caused only a small decrease (7.5%) in the mean open time of channel openings induced by 1 μM ACh, whereas the mean closed time was significantly increased from 200 ± 45 ms to 586 ± 145 ms. The different voltage-dependencies of the two modes of action of these philanthotoxins suggest two binding sites, one deep in the nAChR pore, the other near the extracellular entrance to the pore.

Nicotinic acetylcholine receptors (nAChR) are distributed extensively throughout the central and peripheral nervous systems of vertebrates and invertebrates, where they mediate fast transmission at central synapses and neuromuscular junctions (Corringer et al., 2000; Itier and Bertrand, 2001). The human muscle cell line TE671, which is the subject of this report, expresses nAChR with sequence and subunit stoichiometry [$(\alpha 1)_2\beta 1\gamma\delta$] similar to that of immature human muscle nAChR (Schoepfer et al., 1988; Lukas et al., 1999). The electrophysiological characteristics of TE671 cells, and the nAChR that they express, have been described previously (Oswald et al., 1989; Shao et al., 1998).

Noncompetitive inhibitors of nAChR include antagonists of the open channel conformation of this receptor [e.g., QX-222 (Charnet et al., 1990)] and those that inhibit both closed and open channel conformations [e.g., chlorpromazine (Giraudat et al., 1986)]. These and other noncompetitive inhibitors have been extensively reviewed by Arias (1998). Philanthotoxin-433 (PhTX-433; 4, 3, and 3 indicate the number of methylene groups between the amide/amine groups) (Eldefrawi et al., 1988; Piek and Hue, 1989) is a natural product example of a class of polyamine-containing compounds discovered in certain wasp and spider venoms that noncompetitively antagonize nAChR. In general, natural and synthetic philanthotoxins exhibit properties that are qualitatively similar to those of polyamines, such as spermine and spermidine, but at lower concentrations (Usherwood and Blagbrough, 1991).

PhTX-343 (Fig. 1), a structurally close analog of PhTX-433, is one of many synthetic analogs of the natural product (Anis et al., 1990; Bruce et al., 1990; Karst and Piek, 1991; Karst et al., 1991; Benson et al., 1992, 1993; Strømgaard et al., 1999, 2000; Bixel et al., 2000). It is a potent antagonist of ionotropic glutamate receptors mediating neuromuscular transmission in insects (Eldefrawi et al., 1988; Bruce et al., 1990), of ionotropic glutamate receptors of rat brain (Ragsdale et al., 1989; Jones et al., 1990; Brackley et al., 1993), and of recombinant, ionotropic glutamate receptors from rat (Brackley et al., 1993; Bähring and Mayer, 1998). The interactions of PhTX-433 and PhTX-343 with vertebrate muscle-type

This work was supported by grants from the European Community BIOMED-2 (BMH4-CT97-2395), the Wellcome Trust (067496), and the Danish Medical Research Council (22-00-0372).

ABBREVIATIONS: nAChR, nicotinic acetylcholine receptor; PhTX, philanthotoxin; α-BgTX, α-bungarotoxin; ACh, acetylcholine; MR44, N^1-(3-{[6-({8-[(6-aminohexyl)amino]octyl}amino)hexyl]-amino}propyl)-4-azido-2 hydroxy benzamide.

nAChR have been studied electrophysiologically using frog muscle (Rozental et al., 1989) and the mouse BC_3H1 cell line (Jayaraman et al., 1999) and with neuronal-type nAChR using insect cockroach thoracic ganglia (Rozental et al., 1989) and PC-12 cells (Liu et al., 1997). Biochemical studies of philanthotoxin action on nAChR of *Torpedo nobiliana* electric organ (e.g., Anis et al., 1990) include the use of photosensitive analogs of PhTX-343 (Nakanishi et al., 1997). Recently, Bixel et al. (2000) showed that the photoactive compound N_3-phenyl-PhTX-343-lysine binds to nAChR with a stoichiometry of 2:1 and that a related compound, MR44 (a 3-6-8-6 polyamine linked via an amide group to an aromatic head group), labels, via its aromatic 'head group', the α-subunits of *Torpedo californica* nAChR at a region (Ser-162 to Glu-175) thought to form the outer vestibule of the nAChR channel (Bixel et al., 2001).

It has often been assumed that philanthotoxins, and the structurally related argiotoxins (Jackson and Usherwood, 1988) are exclusively open channel blockers of ionotropic receptors that gate cation-selective ion channels; the pres-

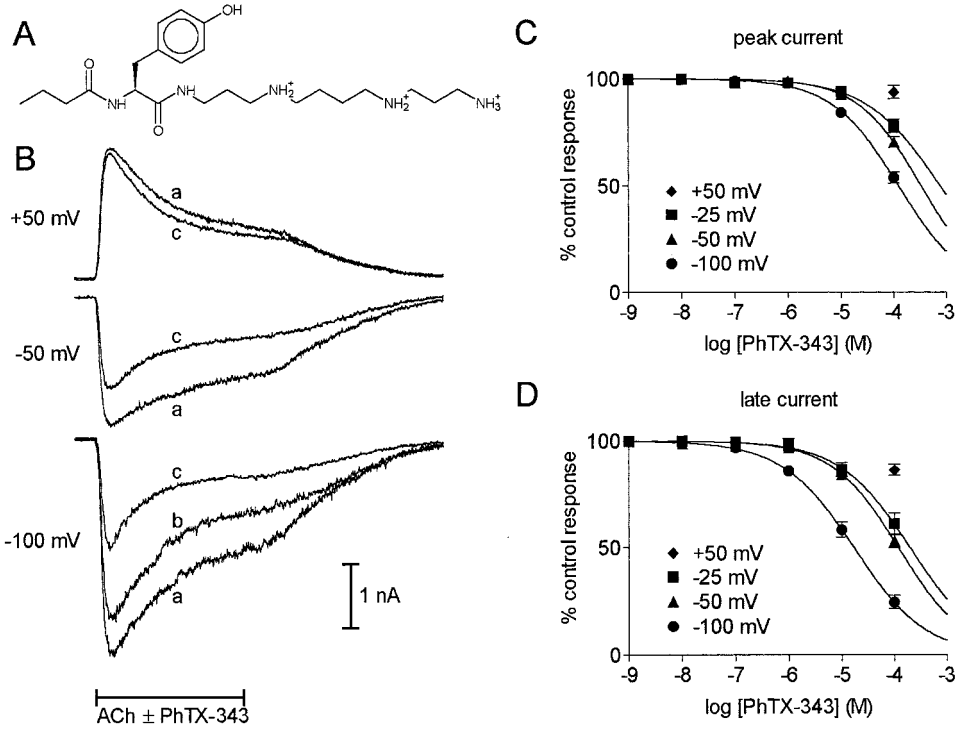

Fig. 1. Inhibition of responses to ACh by coapplied PhTX-343. A, structure of PhTX-343. B, whole-cell currents in response to 2-s applications (indicated by horizontal bar) of 10 μM ACh alone (a) or of ACh coapplied with either 10 μM (b) or 100 μM (c) PhTX-343 at +50 mV, −50 mV, and −100 mV. C and D, concentration-inhibition relationships for PhTX-343 inhibition of peak (C) and late (D) ACh (10 μM)-evoked current at +50 mV (◆, 100 μM PhTX-343 only, n = 17), −25 mV (■, n = 16), −50 mV (▲, n = 45), and −100 mV (●, n = 48). The data are means ± S.E.M. for n cells, and curves are fits of eq. 1. IC_{50} values are given in Table 1.

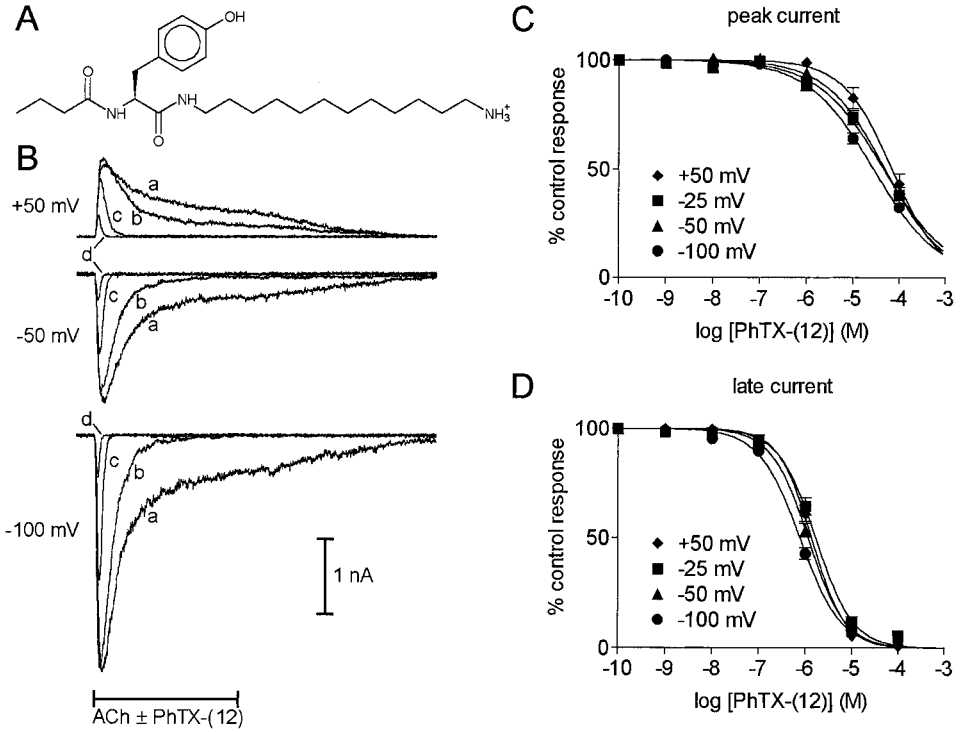

Fig. 2. Inhibition of responses to ACh by coapplied PhTX-(12). A, structure of PhTX-(12). B, whole-cell currents in response to 2-s applications (indicated by horizontal bar) of 10 μM ACh alone (a) or of ACh coapplied with either 1 μM (b), 10 μM (c), or 100 μM (d) PhTX-(12) at +50 mV, −50 mV, and −100 mV. C and D, concentration-inhibition relationships for PhTX-(12) inhibition of peak (C) and late (D) ACh (10 μM)-evoked current at +50 mV (◆, n = 21), −25 mV (■, n = 22), −50 mV (▲, n = 43), and −100 mV (●, n = 45). The data are means ± S.E.M. for n cells, and curves are fits of eq. 1. IC_{50} values are given in Table 1.

ence of multiple positive charges on the polyamine moiety of PhTX-343 is largely responsible for this antagonism. Indeed, a reduction in the number of positive charges reduces antagonism potency by about 10-fold per charge at some receptors (Bruce et al., 1990; Mellor et al., 2003). However, there is substantial evidence that these compounds interact with closed (with potentiation and antagonism) as well as open channel conformations of some classes of excitatory receptor (Jackson and Usherwood, 1988; Usherwood and Blagbrough, 1991; Blagbrough and Usherwood, 1992; Jayaraman et al., 1999; Brier et al., 2002). We have recently shown that removal of either one or both of the secondary amines of PhTX-343, with the consequent reduction in positive charge, enhances rather than reduces antagonist potency at human muscle nAChR (Strømgaard et al., 1999, 2000, 2002; Brier et al., 2002; Mellor et al., 2003); the most potent compound is the dideaza analog PhTX-(12) [the structures of PhTX-343 and PhTX-(12) are shown in Figs. 1 and 2]. In contrast, PhTX-(12) is virtually inactive at insect muscle glutamate receptors (Karst et al., 1991) and at rat α-amino-3-hydroxy-5-methyl-4-isoxazolepropionic acid receptors (Mellor et al., 2003). Here, we show that PhTX-(12) causes largely voltage-independent antagonism of mammalian muscle-type nAChR and increases channel closed time, whereas PhTX-343 causes strong voltage-dependent antagonism and reduces channel open time.

Materials and Methods

PhTX-343 and PhTX-(12). The synthesis of PhTX-343 and PhTX-(12) was described in Strømgaard et al. (1999, 2000) and Wellendorph et al. (2003).

Cell Culture. TE671 cells were cultured as described earlier (Shao et al., 1998). Briefly, they were maintained in Dulbecco's modified Eagle's medium containing 4.5 g/l glucose and supplemented with 10% fetal calf serum, 1 mM pyruvic acid, 2 mM glutamine, 10 IU/ml penicillin, and 10 μg/ml streptomycin (Invitrogen, Carlsbad, CA), and incubated at 37°C in a 5% CO_2 atmosphere. Cells were grown in 25-cm^2 flasks and divided 1:10 when they were approximately 75% confluent. For whole-cell recording, dividing cells were plated onto pieces of glass coverslip (5 × 20 mm) in 35-mm Petri dishes (Nalge Nunc International, Naperville, IL) and transferred 2 to 7 days later to a perfusion bath mounted on the stage of an inverted microscope.

Electrophysiology. Whole-cell preparations and outside-out patches were used to record membrane currents evoked by ACh as described previously (Shao et al., 1998). Briefly, patch pipettes were fabricated from borosilicate glass capillaries (GC150F-10; Clarke Electromedical Instruments, Pangbourne, UK) using a DMZ Universal (Zeitz, Augsburg, Germany) or P-97 (Sutter Instrument Company, Novato, CA) programmable puller. Resistances were ~5 MΩ when the pipettes were filled with either 140 mM CsCl, 1 mM $CaCl_2$, 1 mM $MgCl_2$, 11 mM EGTA, and 5 mM HEPES (for whole-cell recording) or 140 mM KCl, 1 mM $CaCl_2$, 1 mM $MgCl_2$, 11 mM EGTA, and 5 mM HEPES (K^+-pipette solution for outside-out patches); both solutions were pH 7.2. Cells were constantly perfused, at a flow rate of ~10 ml/min, with saline containing 135 mM NaCl, 5.4 mM KCl, 1 mM $CaCl_2$ 1 mM $MgCl_2$, and 5 mM HEPES (adjusted to pH 7.4 with NaOH). Membrane currents were monitored using either an Axopatch 200 (Axon Instruments, Union City, CA) or a L/M-EPC7 patch-clamp amplifier (List Electronic, Darmstadt, Germany). Agonist/antagonists were applied as 1- to 8-s (whole-cell) or 10- to 30-s (outside-out patches) pulses using a DAD-12 Superfusion system. The patch-clamp amplifier and DAD-12 Superfusion system were controlled by pClamp 5.7.2 software (Axon Instruments), which simultaneously acquired data to the hard disk of an IBM-compatible PC. Experiments were performed at 18 to 22°C. Chemicals were purchased from the Sigma Chemical Co. (St. Louis, MO)

Analyses. Data analyses were undertaken on an IBM-compatible PC using pClamp 5.7.2 software (Axon Instruments) for whole-cell data or Strathclyde Electrophysiology Software WinEDR2.3.3 (Dr. J. Dempster, Department of Physiology and Pharmacology, University of Strathclyde, UK) for single-channel data. Curve fitting was performed using Graphpad Prism software. IC_{50} (EC_{50}) values were estimated by fitting the following equation to concentration-inhibition (-response) (%) data:

$$\%\ \text{control response} = \frac{M}{1 + (IC_{50}/[PhTX]^{n_H})} \quad (1)$$

where M is the maximum response and n_H is the Hill slope. Inhibition-voltage data were fitted by a variation of the Woodhull equation (Woodhull, 1973):

$$\frac{I}{I_0} = \frac{M}{1 + [PhTX]/K_{d(0)}\exp(-V_H z \delta F/RT)} \quad (2)$$

where I_0 is the current in the absence of PhTX-343, I is the current in the presence of PhTX-343, M is the maximum fractional current (I/I_0) in the presence of PhTX-343 (to account for any voltage-independent antagonism), $K_{d(0)}$ is the dissociation constant at 0 mV, z is the valence of the blocking molecule, δ is the fraction of the membrane electric field traversed by PhTX-343, F is Faraday's constant, R is the gas constant, and T is absolute temperature. Rates of onset of inhibition were determined by fitting exponential decays to current versus time data after the addition of antagonist during steady-state current evoked by 10 μM ACh. Desensitization rates were determined by fitting exponential decays to the decaying phase of current versus time data.

Values for P were determined using unpaired or paired (where appropriate) Student's t test; differences between data sets were considered significant for $P < 0.05$. In experiments comparing inhibition under varying conditions of time, preapplication, and ACh concentration, paired measurements have been obtained from each cell and repeated for n cells. This allows for more accurate interpretation of the results that could otherwise be influenced by cell-to-cell variation. In all other experiments, large n values were employed.

TABLE 1

IC_{50} values for inhibition of peak and late whole-cell currents induced by 10 μM ACh during its co-application with either PhTX-343 or PhTX-(12) at +50, −25, −50, and −100 mV

For all comparisons of peak and late currents, V_H values, or PhTX-343 and PhTX-(12), $P < 0.0001$ (unpaired Student's t test). Values are presented as mean ± S.E.M. (n cells).

	+50 mV	−25 mV	−50 mV	−100 mV
		μM		
PhTX-343				
Peak current		774 ± 139 (16)	333 ± 32 (45)	124 ± 7 (48)
Late current		200 ± 14 (16)	120 ± 7 (45)	17.2 ± 0.3 (48)
PhTX-(12)				
Peak current	70.5 ± 2.8 (21)	46.9 ± 5.4 (22)	49.7 ± 2.8 (43)	28.2 ± 1.9 (45)
Late current	1.37 ± 0.12 (21)	1.67 ± 0.14 (22)	1.16 ± 0.06 (43)	0.77 ± 0.05 (45)

Results

Coapplication of ACh and Philanthotoxins. Responses of TE671 cells to application of ACh (>1 μM) are characterized by a current [inward at negative holding potential (V_H)] that rises to a peak before rapidly decaying to a plateau because of desensitization (Fig. 1). Recovery from desensitization is complete within 30 s (Shao et al., 1998). The effects of PhTX-343 and PhTX-(12) were assessed by analyzing: 1) the peak current obtained in the presence and absence of the philanthotoxins (peak current data); and 2) the late current (1 s after the commencement of ACh application) obtained in the presence and absence of philanthotoxin (late current data). The measurement of peak and late currents enabled an assessment of time-dependent antagonism by the two compounds. After 1 s, the nAChR population consists of channels in their open, desensitized, or closed states, the relative proportions of which determine the amplitude of the late current relative to the peak current. Because these proportions may vary from cell to cell, steps were taken (see *Materials and Methods*) to avoid misinterpretations resulting from the fact that PhTX-343 and PhTX-(12) may only bind to certain receptor states.

Concentration Dependence. Concentration-inhibition relationships for PhTX-343 and PhTX-(12) were obtained at +50 mV, −25 mV, −50 mV, and −100 mV by applying 2-s pulses of 10 μM ACh, with or without philanthotoxin (10 pM to 100 μM), at 30-s intervals (Fig. 1). IC_{50} values were calculated by fitting eq. 1 to the concentration-inhibition data (Table 1). The IC_{50} values for PhTX-343 were voltage-dependent; i.e., the values for inhibition of both peak and late currents were lower at −100 mV than at −25 mV. Overall, PhTX-343 caused little inhibition at +50 mV (Fig. 1), and it was not possible to estimate an IC_{50} for this V_H. Antagonism by PhTX-343 at negative V_H was time-dependent; the IC_{50} for peak current inhibition was greater than that for late current inhibition (Fig. 1). PhTX-(12) was more effective than PhTX-343 at inhibiting the peak and late currents (Fig. 2); i.e., peak current inhibition by PhTX-(12) was 16.5-, 6.7-, and 4.4-fold more potent than by PhTX-343, and late current inhibition by PhTX-(12) was 120-, 103-, and 22-fold more potent than by PhTX-343, at −25, −50, and −100 mV, respectively (data based on IC_{50} values). The IC_{50} values for inhibition by PhTX-(12) at +50 mV and −100 mV were significantly different ($P < 0.0001$), for both peak and late current (Table 1). However, in contrast to PhTX-343, potent inhibition by PhTX-(12) was observed at +50 mV (Table 1; Fig. 2). In common with PhTX-343, antagonism by PhTX-(12) was time-dependent, inhibition of the late current being greater than that of the peak current (Fig. 2).

Competition with ACh. The possibility that PhTX-343 and/or PhTX-(12) competes with ACh was investigated 1) by determining the effect of ACh concentration on the concentration-inhibition relationships for the philanthotoxins and 2) by determining the effect of the philanthotoxins on the concentration-response relationship for ACh. Because the rate of rise and decay of the peak ACh-induced current depends on ACh concentration, the late current induced by the agonist was used in these studies. When the ACh concentration was raised from 10 μM to 1 mM, the IC_{50} value for late current inhibition by PhTX-343 at −50 mV was unchanged (Fig. 3, A and B). Also, the IC_{50} values for PhTX-(12) at +50, −50, and −100 mV with 10 μM ACh were not different from those obtained with 1 mM ACh (Fig. 3, C and D).

There was no change in percentage inhibition by 100 μM PhTX-343 at −50 mV and −100 mV when the ACh concentration was increased in steps from 1 μM to 1 mM (Fig. 3E). Inhibition by 10 μM PhTX-(12) at −50 mV and −100 mV increased ($P = 0.0139$ for −50 mV, but 0.0800 for −100 mV) when the ACh concentration was raised from 1 to 10 μM and remained unchanged above this (Fig. 3E). It follows from these data that there is no competition between PhTX-343 or PhTX-(12) and ACh. Interestingly, the small enhancement of inhibition by the philanthotoxin that was seen when the ACh concentration was raised from 1 to 10 μM coincided with a major increase in desensitization by the agonist.

Voltage Dependence. The influence of V_H on the action of PhTX-343 was studied quantitatively by applying 2-s pulses of 10 μM ACh, with or without philanthotoxin, at voltage steps (−25 mV) between +50 mV and −125 mV. Peak current inhibition by 100 μM PhTX-343 was not significant

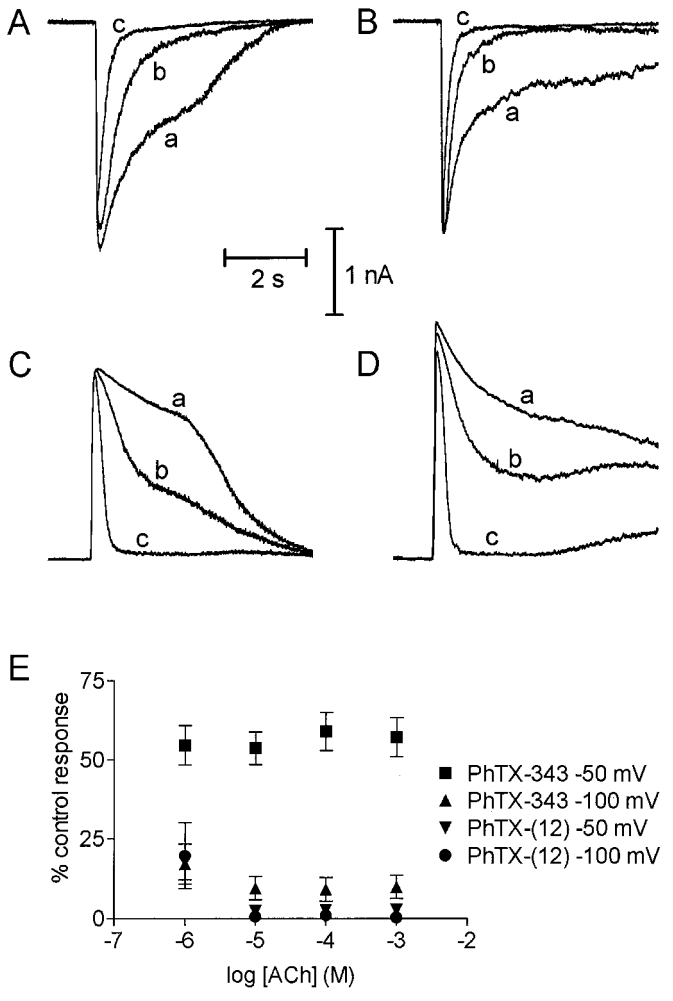

Fig. 3. Effect of ACh concentration on inhibition by PhTX-343 and PhTX-(12). A and B, whole-cell currents in response to 10 μM ACh (A) or 1 mM ACh (B), either alone (a) or with 10 μM (b) or 100 μM (c) PhTX-343 at −100 mV. C and D, whole-cell currents in response to 10 μM ACh (C) or 1 mM ACh (D) either alone (a) or with 1 μM (b) or 10 μM (c) PhTX-(12), at +50 mV. Horizontal bars indicate the 2-s application of ACh ± toxin. E, plots of inhibition versus ACh concentration for 100 μM PhTX-343 at −50 mV (■, $n = 10$) and −100 mV (▲, $n = 9$) and 10 μM PhTX-(12) at −50 mV (▼, $n = 10$) and −100 mV (●, $n = 10$). The data are mean ± S.E.M. of n cells.

(6.9 ± 7.1%) at +50 mV but reached 71.9 ± 5.9% at −125 mV (n = 13). Late current inhibition by 100 μM PhTX-343 increased from 12.1 ± 5.6% at +50 mV to 96.5 ± 2.3% at −125 mV (n = 13) (Fig. 4A). By fitting eq. 2 to plots of fractional inhibition of peak and late currents by 100 μM PhTX-343 against V_H, estimates for $z\delta$ and M were obtained (Fig. 4A). Assuming that the valence of PhTX-343 is +3 at physiological pH (Strømgaard et al., 1999), the δ-values for peak and decay current inhibition by 100 μM PhTX-343 were 0.15 ± 0.02 and 0.35 ± 0.04, respectively (n = 13). M values for peak and late current inhibition by PhTX-343 were 1.08 ± 0.06 (n = 13) and 0.92 ± 0.03 (n = 13), respectively (significantly different from unity for late current; P = 0.0334). These data lend further support to the conclusion that antagonism of ACh responses by PhTX-343 is largely voltage-dependent. Antagonism by PhTX-(12) is shown for comparison at +50, −25, −50, and −100 mV in Fig. 4B. Although inhibition by this philanthotoxin was slightly greater at −100 mV than at +50 mV ($P < 0.0004$), it was not possible to fit eq. 2 to estimate δ values. Thus, we conclude that inhibition by PhTX-(12) is only weakly voltage-dependent.

Preapplication of Philanthotoxin. Inhibition of the ACh-induced current was increased by preapplying either PhTX-343 or PhTX-(12) before these philanthotoxins were coapplied with ACh, with no interval between the pre- and coapplication (Fig. 5). Maximum enhancement of inhibition by both PhTX-343 and PhTX-(12) was obtained with a >1-s preapplication (Fig. 6A). Consequently, we have used 30-s preapplications of philanthotoxin (at +50 mV, −50 mV, and −100 mV; toxin concentrations, 1, 10, and 100 μM) (Table 2). Solution exchange was completed within 50 ms. Therefore, the observed enhancement of inhibition was not caused by equilibration of philanthotoxin at the cell membrane.

In general, inhibition of both peak and late currents was increased with preapplication of the two philanthotoxins, although inhibition of the late current remained greater than that of the peak current (Table 2; Figs. 5 and 6), indicating that inhibition was dependent on nAChR activation. The rates of decay of responses to 10 μM ACh plus either 100 μM PhTX-343 or 1 μM PhTX-(12), without and with preincubation of the philanthotoxins, were ascertained at +50 mV (to eliminate voltage-dependent antagonism). With 100 μM PhTX-343, the decay rate increased from 1.23 ± 0.22/s without preapplication to 3.35 ± 0.23/s with preapplication (n = 11, $P < 0.0001$) (Fig. 6B); with 1 μM PhTX-(12), the decay rate increased from 1.48 ± 0.20 to 4.03 ± 0.50/s (n = 10, $P <$ 0.0001) (Fig. 6C).

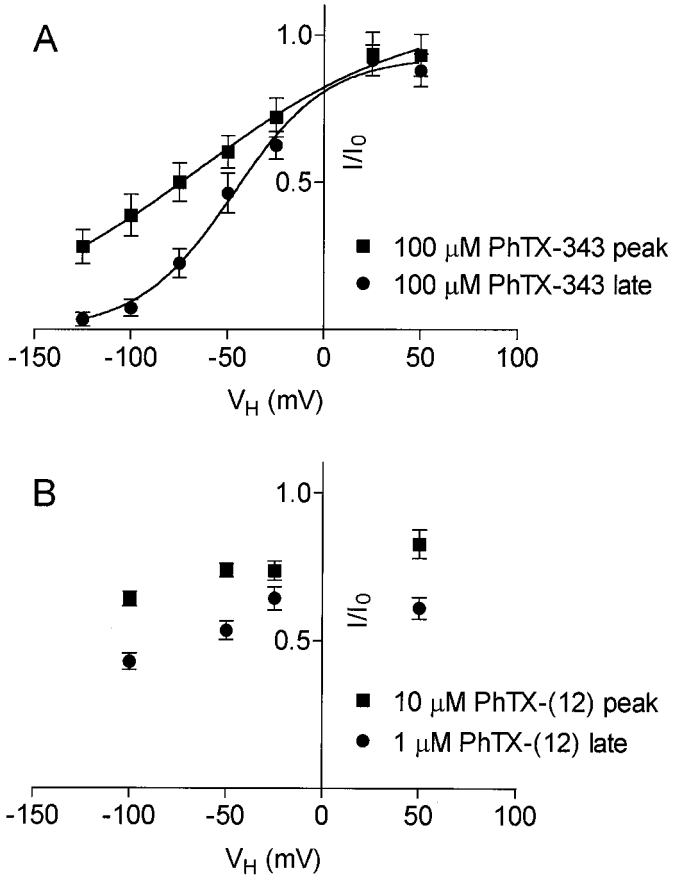

Fig. 4. Voltage-dependence of inhibition by PhTX-343 and PhTX-(12). A, fraction of control response (I/I_0) versus V_H for inhibition by 100 μM PhTX-343 (n = 13) of ACh (10 μM)-evoked peak current (■) and late current (●). The data are fit by eq. 2 (curves) giving $z\delta$ = 0.45 ± 0.05 and 1.04 ± 0.12, M = 1.08 ± 0.06 and 0.92 ± 0.03, and $K_{d(0)}$ = 321 ± 85 μM and 690 ± 216 μM for peak and late current data, respectively. B, fraction of control response (I/I_0) versus V_H for inhibition of ACh-(10 μM) evoked peak current by 10 μM PhTX-(12) (■) and late current by 1 μM PhTX-(12) (●) (n = 21–45). The data are mean ± S.E.M. of n cells.

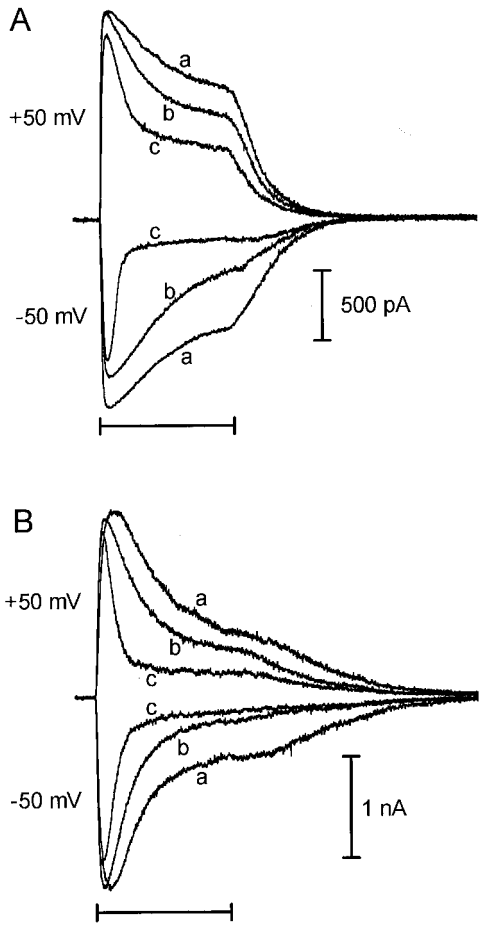

Fig. 5. Preapplication of PhTX-343 and PhTX-(12). Whole-cell currents in response to 10 μM ACh alone (a), coapplied with toxin (b) or coapplied with toxin after a 30-s preincubation with toxin alone, for 100 μM PhTX-343 (A) and 1 μM PhTX-(12) (B). Responses are shown at +50 mV and −50 mV. Horizontal bars indicate the 2-s application of ACh ± toxin.

Application of Philanthotoxin during the ACh-Induced Current. The kinetics of antagonism by PhTX-343 and PhTX-(12) were investigated by applying the philanthotoxins during the "steady-state" current induced by ACh. ACh (10 μM) was applied for a period of 4 s, followed by 10 μM ACh with either PhTX-343 or PhTX-(12) for 2 s, followed by 10 μM ACh for 2 s. This approach was only possible with TE671 cells that exhibited a pronounced late current during application of ACh. The above protocol was repeated at +50, −50, and −100 mV. Antagonism of the "steady-state" current by PhTX-343 was voltage-dependent, with no antagonism at +50 mV, even at 100 μM PhTX-343 (Fig. 7A). At −50 mV, inhibition was obtained only with 100 μM PhTX-343, but at −100 mV, substantial inhibition occurred with 10 μM PhTX-343. Inhibition of the "steady-state" current was obtained with 1 μM PhTX-(12), even at +50 mV, with inhibition being largely unaffected by V_H (Fig. 7B).

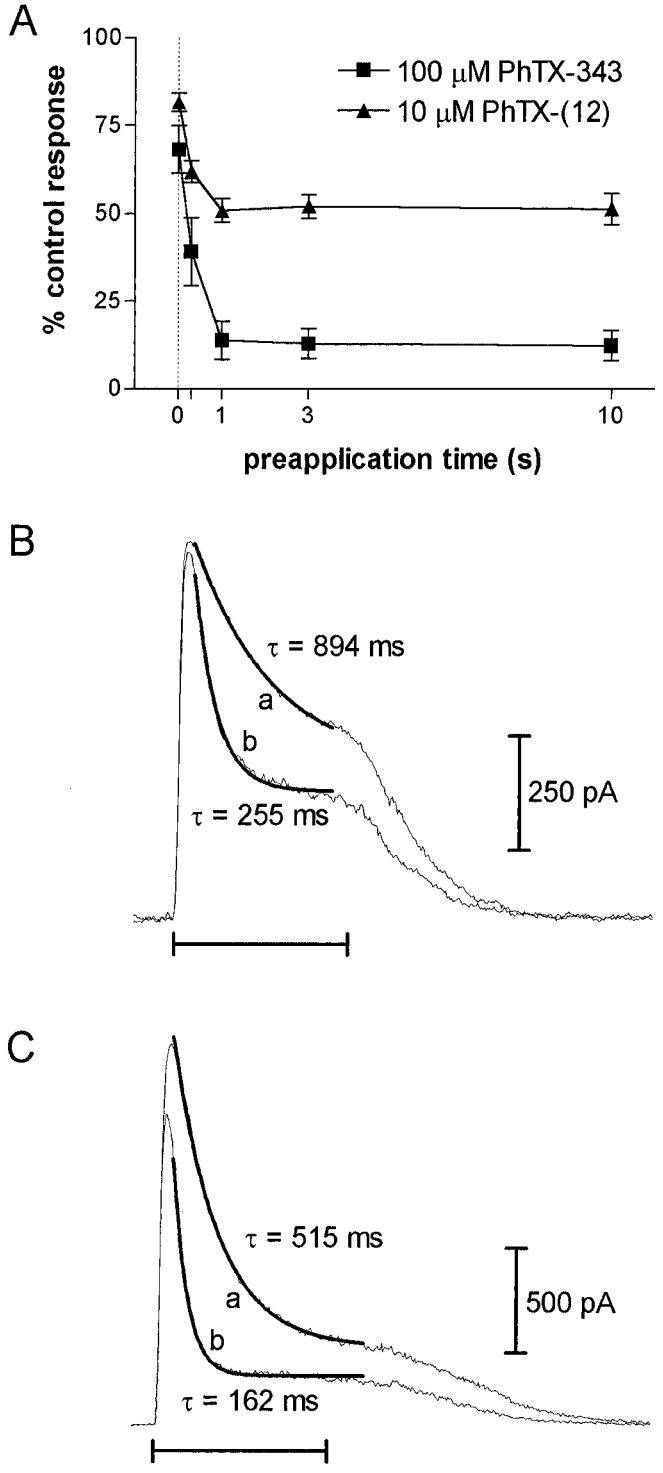

Fig. 6. Preapplication of PhTX-343 and PhTX-(12). A, plots of inhibition versus preapplication time for inhibition of peak current by 100 μM PhTX-343 (■) or 10 μM PhTX-(12) (▲) at −100 mV. B and C, whole-cell current responses to 10 μM ACh coapplied with either 100 μM PhTX-343 (B) or 1 μM PhTX-(12) (C) without (a) and with (b) a 30-s preapplication at +50 mV. The decay phase of each response is fitted by a single exponential (thick curve). Horizontal bars indicate the 2-s application of ACh + toxin.

Onset Rates. The onset rates of inhibition of the ACh-induced current by PhTX-343 and PhTX-(12) were estimated from best-fits of exponentials to the onset phases of inhibition of "steady state" currents. The rates were corrected for the presence of any residual, ACh-induced desensitization. Inhibition onsets for PhTX-343 were best fitted by double exponentials comprising fast and slow components (Fig. 7A, Table 3). The fast rate for PhTX-343 was independent of V_H, but the slow rate was higher at more negative V_H [0.16 ± 0.12/s (n = 6) at −50 mV and 1.43 ± 0.45/s (n = 8) at −100 mV (P = 0.0373)]. However, the fast onset rate was limited by the rate at which the philanthotoxin could be exchanged. Inhibition onsets for PhTX-(12) were best-fitted with a single exponential (Fig. 7B, Table 3) and were voltage-independent.

Recovery from Inhibition by PhTX-343 and PhTX-(12). Rates of recovery from inhibition were determined by fitting exponentials to the recovery phases of inhibition elicited by applying the philanthotoxins during "steady-state" currents induced by ACh (Fig. 7; Table 3). Recovery rates were higher with lower PhTX-343 concentrations and at less negative V_H. Recovery from inhibition by PhTX-(12) was slower than for PhTX-343, with a weak dependence on antagonist concentration at −50 mV (P = 0.0278). There was also a weak dependence on V_H; recovery was faster at +50 mV than at −50 mV. In some cells held at −100 mV, recovery from 100 μM PhTX-(12) was barely detectable.

Recovery from inhibition by PhTX-343 and PhTX-(12) was also investigated by applying a 2-s pulse of 10 μM ACh 30 s after coapplication of 10 μM ACh with 100 μM philanthotoxin (Fig. 8). A 2-s pulse of 10 μM ACh was applied 30 s before the coapplication step, as control. The experiment was repeated at −50 and −100 mV for PhTX-343 and at +50, −50, and −100 mV for PhTX-(12). Table 4 summarizes the results of the experiment. Both peak and late currents recovered by >66% after inhibition by 100 μM PhTX-343; recovery of the peak current was voltage-dependent. At −100 mV, recovery of the late current was greater than that of the peak current (Fig. 8A). Recovery of the peak and late currents after inhibition by PhTX-(12) was slower than after application of PhTX-343 (Table 4). The rates of recovery of peak and late currents were not significantly different. Recovery from PhTX-(12) antagonism was voltage-dependent with significantly greater recovery at +50 mV (Fig. 8B). Recovery of peak and late currents was not enhanced by stepping V_H from −100 to +50 mV for 26 s in the absence of agonist (Fig. 8C).

Single Channel Studies. Outside-out patches from TE671 cells were exposed to 1 μM ACh for 10 to 30 s in either the absence or presence of philanthotoxin [10 μM PhTX-343

or 1 μM PhTX-(12)] at −60 mV (potassium channels present in outside-out patches from TE671 cells reverse at this V_H with the high K^+-containing pipette solution). Measurements of the effects of the philanthotoxins on single-channel activity were made when channel open probability had reached a constant value (i.e., when desensitization of nAChR had reached a steady state). The effects of coapplying PhTX-343 or PhTX-(12) with ACh are illustrated in Fig. 9 and Table 5. PhTX-343 reduced the mean open time (m_o), whereas PhTX-(12) increased the mean closed time (m_c). The mean single-channel conductance (G) was not significantly affected by either PhTX-343 or PhTX-(12) (Fig. 9, F–H; Table 5); no subconductance levels were evident in either the absence or the presence of the philanthotoxins. The open-state peak of the all-points histogram for channel openings in the presence of PhTX-343 (Fig. 9G) was skewed toward the closed-state peak because of attenuated brief events and could not be accurately fit with a Gaussian distribution. The effects of PhTX-343 and PhTX-(12) on m_c were voltage-independent, whereas the large reductions in m_o that were obtained with PhTX-343 were highly voltage-dependent.

Discussion

This study has shown that PhTX-343 noncompetitively inhibits the muscle-type nAChR of TE671 cells in a voltage-dependent manner. Like Liu et al. (1997), we have shown that late current inhibition by PhTX-343 is greater than peak current inhibition. This time-dependent antagonism implies that interaction of PhTX-343 with nAChR is slow and/or that

TABLE 2

Inhibition of peak and late whole-cell currents induced by 10 μM ACh without (C) or with (P) a 30-s preapplication by either PhTX-343 or PhTX-(12) at + 50, −50, and −100 mV

All p values from unpaired Student's t test. Values are presented as mean ± S.E.M. (n cells).

	Control Response					
	+50 mV		−50 mV		−100 mV	
	Peak Current	Late Current	Peak Current	Late Current	Peak Current	Late Current
	%					
PhTX-343						
1 μM						
C	96.3 ± 1.6 (13)	92.8 ± 2.7 (13)	99.4 ± 2.0 (12)	97.3 ± 1.7 (12)	99.1 ± 3.3 (10)	94.0 ± 2.9 (10)
P	85.1 ± 3.5 (13)**	45.3 ± 3.8 (13)***†††	91.4 ± 4.3 (12)	66.8 ± 4.8 (12)***†††	86.8 ± 3.7 (10)*	57.1 ± 5.2 (10)***†††
10 μM						
C	98.4 ± 1.9 (13)	89.7 ± 1.9 (13)††	92.9 ± 2.4 (12)	84.4 ± 2.8 (12)†	93.6 ± 3.1 (10)	46.7 ± 8.1 (10)†††
P	79.9 ± 3.1 (13)***	40.9 ± 3.6 (13)***†††	79.7 ± 5.0 (12)*	49.5 ± 4.4 (12)***†††	68.1 ± 8.2 (10)**	12.1 ± 5.6 (10)**†††
100 μM						
C	90.1 ± 3.6 (13)	84.8 ± 3.4 (13)	78.3 ± 3.2 (20)	58.5 ± 3.4 (20)†††	66.9 ± 6.5 (12)	23.5 ± 8.3 (12)†††
P	70.1 ± 6.7 (13)*	47.5 ± 5.2 (13)***†	39.6 ± 5.1 (20)***	24.7 ± 3.0 (20)***†	13.8 ± 5.8 (12)***	4.82 ± 2.52 (12)*
PhTX-(12)						
1 μM						
C	104.7 ± 3.4 (10)	73.2 ± 3.3 (10)†††	98.4 ± 2.2 (10)	67.7 ± 3.4 (10)†††	101.0 ± 2.8 (10)	65.1 ± 4.5 (10)†††
P	92.8 ± 4.2 (10)*	42.0 ± 5.5 (10)***†††	88.7 ± 3.6 (10)*	40.5 ± 4.6 (10)***†††	91.3 ± 3.1 (10)*	37.6 ± 5.3 (10)***†††
10 μM						
C	94.7 ± 2.4 (15)	12.1 ± 1.8 (15)†††	89.3 ± 1.3 (13)	5.58 ± 2.26 (13)†††	88.5 ± 3.4 (10)	2.49 ± 1.51 (10)†††
P	86.3 ± 2.7 (15)*	8.44 ± 1.07 (15)†††	78.6 ± 3.2 (13)**	1.56 ± 0.77 (13)†††	74.6 ± 4.8 (10)*	0.29 ± 0.11 (10)†††
100 μM						
C	68.8 ± 10.7 (11)	0.34 ± 0.52 (11)†††	62.4 ± 5.8 (10)	4.30 ± 3.06 (10)†††	65.6 ± 5.8 (11)	4.07 ± 2.86 (11)†††
P	25.1 ± 5.1 (11)**	0.04 ± 0.11 (11)†††	9.01 ± 1.93 (10)***	0.21 ± 0.20 (10)†††	3.83 ± 0.67 (11)***	0.79 ± 0.35 (11)†††

* ($P < 0.05$), ** ($P < 0.01$), and *** ($P < 0.001$) indicate significance of increase in inhibition with preapplication.
† ($P < 0.05$), †† ($P < 0.01$), and † ($P < 0.001$) indicate significance of difference between peak and late current inhibition.

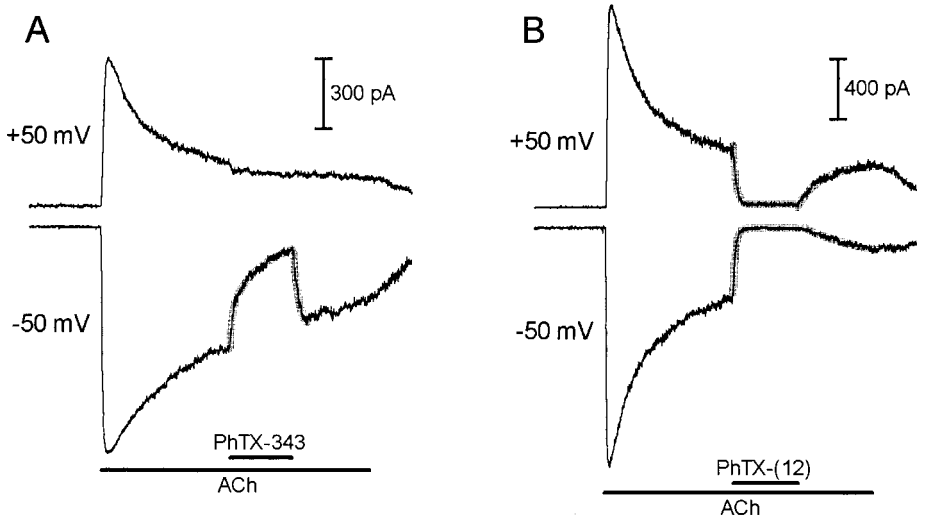

Fig. 7. Application of PhTX-343 or PhTX-(12) during a response to ACh. Either 100 μM PhTX-343 (A) or 10 μM PhTX-(12) (B) was coapplied for 2 s, 4 s after the start of an 8-s response to 10 μM ACh, at +50 mV and −50 mV. The gray lines are fits of double (PhTX-343) or single [PhTX-(12)] exponential decays (antagonizing phase) or exponential associations (recovery phase).

antagonism of nAChR by PhTX-343 involves processes subsequent to receptor activation. The IC_{50} values for late current inhibition by PhTX-343 described herein are near the estimates of PhTX-343 potency in binding studies on *Torpedo* sp. nAChR; IC_{50} values of 50 μM (Nakanishi et al., 1997) and 2.6 μM (Anis et al., 1990) for displacement of [^{3}H]histrionicotoxin from *Torpedo* sp. nAChR by PhTX-343 have been reported. The noncompetitive nature of philanthotoxin inhibition of nAChR is supported by Bixel et al. (2000), who showed that the binding of N_3-Ph-PhTX-343-Lys to resting

TABLE 3

Onset and recovery rates for inhibition of steady-state whole-cell current induced by 10 μM ACh at +50, −50, and −100 mV. All p values are from unpaired Student's t test. Values are presented as mean ± S.E.M. (n cells).

	+50 mV	−50 mV	−100 mV
Onset rate (s^{-1})			
PhTX-343			
10 μM			
Fast			17.8 ± 2.7 (7)
Slow			1.10 ± 0.28 (7)
100 μM			
Fast		20.0 ± 2.4 (6)	18.1 ± 3.1 (8)
Slow		0.16 ± 0.12 (6)	1.43 ± 0.45 (8)†
PhTX-(12)			
1 μM	0.53 ± 0.15 (6)	0.61 ± 0.13 (9)	1.08 ± 0.22 (8)
10 μM	8.13 ± 0.64(6)***	7.46 ± 1.15(9)***	8.03 ± 1.49(9)***
100 μM	17.7 ± 1.7 (6)***	13.3 ± 2.1 (9)*	14.0 ± 2.4 (9)
Recovery rate (s^{-1})			
PhTX-343			
10 μM			8.79 ± 3.22 (5)
100 μM		11.7 ± 3.1 (7)	4.15 ± 1.23 (7)†
PhTX-(12)			
1 μM	1.62 ± 0.27 (5)†	0.84 ± 0.13 (9)	0.86 ± 0.19 (6)
10 μM	1.31 ± 0.09(6)†††	0.55 ± 0.06 (10)	0.65 ± 0.09 (8)
100 μM	1.08 ± 0.10(6)†††	0.40 ± 0.09 (6)[a]	0.36 ± 0.10 (3)

* ($P < 0.05$) and *** ($P < 0.001$) indicate significance of difference from the effect of the previous concentration of philanthotoxin.
† ($P < 0.05$) and ††† ($P < 0.001$) indicates significance of difference from values at −50 mV.
[a] $P < 0.05$ indicates significant difference from the effect at 1 μM philanthotoxin.

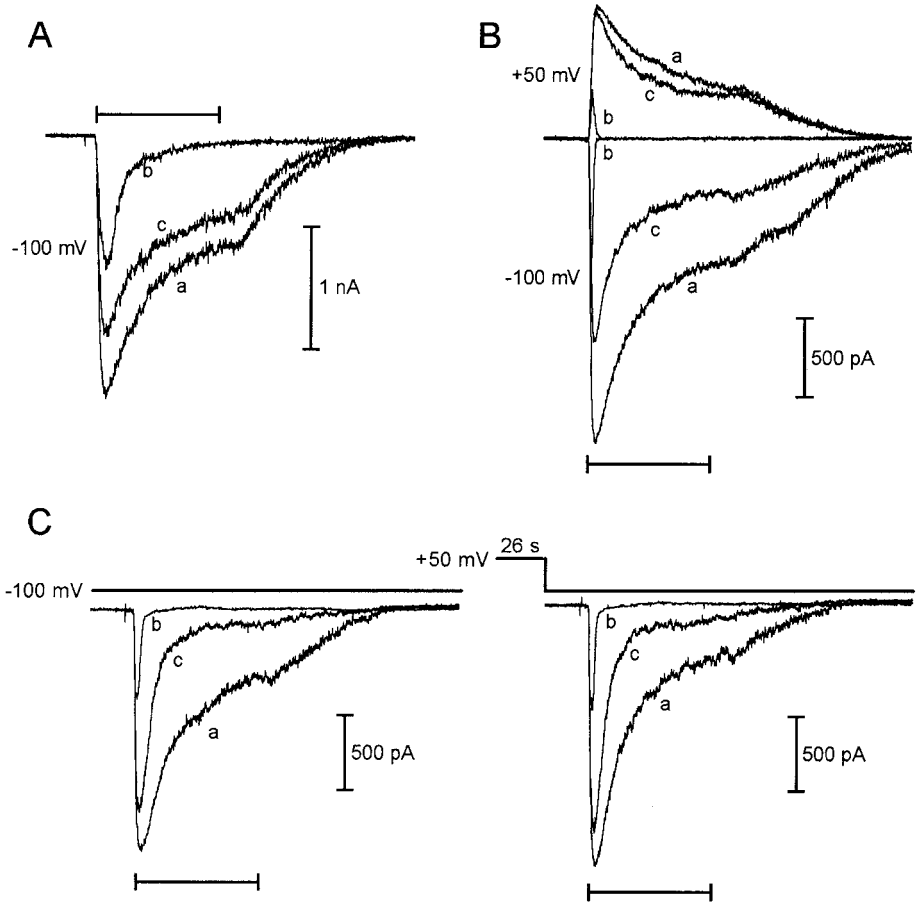

Fig. 8. Recovery from antagonism by PhTX-343 and PhTX-(12). A and B, whole-cell currents in response to 10 μM ACh alone before (a) and 30 s after (c) inhibition (b) by either 100 μM PhTX-343 (A) or PhTX-(12) (B). C, whole-cell currents in response to 10 μM ACh alone before (a) and 30 s after (c) inhibition (b) by 100 μM PhTX-(12) at −100 mV, without (left) or with (right) a 26-s pulse to +50 mV between b and c. Both datasets in C are from the same cell. Horizontal bars indicate the 2-s application of ACh ± toxin.

state *Torpedo californica* nAChR is unaffected by the presence of α-BgTX and slightly enhanced by the presence of carbamylcholine. Bixel et al. (2001) also showed that binding of a related philanthotoxin, ^{125}I-MR44, was largely unaffected by either α-BgTX or carbamylcholine. Previously, however, Rozental et al. (1989) reported that very high concentrations of PhTX-433 inhibited the binding of both ACh and α-BgTX to *Torpedo* sp. nAChR.

The voltage-dependence of inhibition by PhTX-343 is in accordance with the results of Rozental et al. (1989) who demonstrated that inhibition of frog muscle end-plate current by the natural product PhTX-433 is voltage-dependent. Voltage-dependent antagonism of neuronal-type nAChR by PhTX-343 has also been demonstrated (Liu et al., 1997). PhTX-343 is trivalent at physiological pH with all three of its amino groups positively charged (Jaroszewski et al., 1996). It follows that if PhTX-343 blocks the ion channel pore of nAChR, then its activity should be influenced by the transmembrane electric field. The conclusion that PhTX-343 blocks the open channel gated by nAChR is supported by the reduction of m_o in our single-channel studies. The positively charged amino groups may interact with negatively charged or nucleophilic residues within the nAChR channel. It is suggested that the two hydrophilic rings containing serine, asparagine and threonine residues and the negatively charged intermediate and internal rings (Brier et al., 2002) form a binding site for the polyamine chain of PhTX-343. The more hydrophobic extracellular region of the pore would then accommodate the hydrophobic 'head' of PhTX-343. Although the δ-values calculated from the voltage dependence of antagonism might suggest a shallower binding site in the pore, these values should be treated with caution, because PhTX-343 is a complex, elongated organic cation with distributed charge [unlike protons, for which the Woodhull (1973) analysis was developed] and may also be subject to internal hydrogen bonding (Tikhonov et al., 2000). The IC_{50} values for peak current inhibition by PhTX-343 are much higher than the reported value of ~100 nM (at $V_H = -60$ mV) for peak current inhibition by PhTX-343 of the neuronal-type nAChR of PC-12 cells (Liu et al., 1997). It is likely that γ and δ subunits, which are found only in muscle nAChR, are responsible for this difference in sensitivity to PhTX-343, although differences in the α1 and β1 subunits of the two types of nAChR cannot be ruled out. The γ and δ subunits introduce lysine residues (positive charges) to the external mouth of the pore, whereas the α and β subunits contribute negative charges in the form of glutamate and aspartate residues. The presence of lysine residues in the muscle-type nAChR would reduce the probability of PhTX-343 entering the pore. Second, the γ subunit has a glutamine instead of a glutamate (as with α, β, and δ) and, perhaps more importantly, a lysine instead of an aspartate (as with α, β, and δ) at the intermediate and internal rings, respectively.

When PhTX-343 was preapplied, a significant voltage-independent antagonism was uncovered, suggesting that this philanthotoxin also interacts with the closed channel conformation of nAChR. The inhibition of late current at +50 mV and the small increase in m_c in the single-channel studies lend support to this conclusion. Jayaraman et al. (1999) previously identified open- and closed-channel antagonism for PhTX-343 in their study of mouse adult muscle nAChR of BC_3H1 cells. The enhancement of inhibition by PhTX-343 that resulted from preapplication of the antagonist was characterized by an increase in the rate of decay of the ACh-induced current, which could be interpreted as an increase in the rate of desensitization.

PhTX-(12) was more potent than PhTX-343, and the IC_{50} values for peak and decay current inhibition by PhTX-(12) were largely unaffected by changes in V_H. Like that for PhTX-343, the action of PhTX-(12) was time-dependent; late

TABLE 4

Recovery from inhibition by co-applied 100 μM PhTX-343 or 100 μM PhTX-(12) of whole-cell currents induced by 10 μM ACh at + 50, −50, and −100 mV.

All *P* values are from unpaired Student's *t* test. Values are presented as mean ± S.E.M. (*n* cells).

Toxin	Recovery		
	+50 mV	−50 mV	−100 mV
		%	
PhTX-343 (100 μM)			
Peak current		78.6 ± 3.8 (48)	66.6 ± 4.4 (46)*
Late current		80.3 ± 3.2 (48)	78.3 ± 2.8 (46)†
PhTX-(12) (100 μM)			
Peak current	87.1 ± 5.8 (11)	74.2 ± 3.9 (26)	53.3 ± 3.9 (23)***
Late current	86.8 ± 5.6 (11)**	64.4 ± 4.0 (26)	48.5 ± 4.2 (23)**

* ($P < 0.05$), ** ($P < 0.01$), and *** ($P < 0.001$) indicate significance of difference from data obtained at −50 mV.
† ($P < 0.05$) indicates significance of difference between recovery of peak and late currents.

TABLE 5

Single-channel parameters for currents induced by 1 μM ACh in outside-out patches obtained in the absence (control) and presence (toxin) of 10 μM PhTX-343 or 1 μM PhTX-(12)

	P_o	m_o	m_c	G
		ms	*ms*	*pS*
PhTX-343 ($n = 11$)				
Control	0.048 ± 0.014	4.42 ± 0.44	178 ± 38	35.7 ± 0.9
Toxin	0.018 ± 0.006**	1.58 ± 0.10***	225 ± 55	33.5 ± 0.9
PhTX-(12) ($n = 9$)				
Control	0.034 ± 0.012	4.40 ± 0.46	200 ± 45	35.9 ± 1.1
Toxin	0.017 ± 0.008**	4.14 ± 0.45	586 ± 145*	35.6 ± 1.1

* ($P < 0.05$), ** ($P < 0.01$), and *** ($P < 0.001$) indicate significance of difference from control values (paired Student's *t* test).

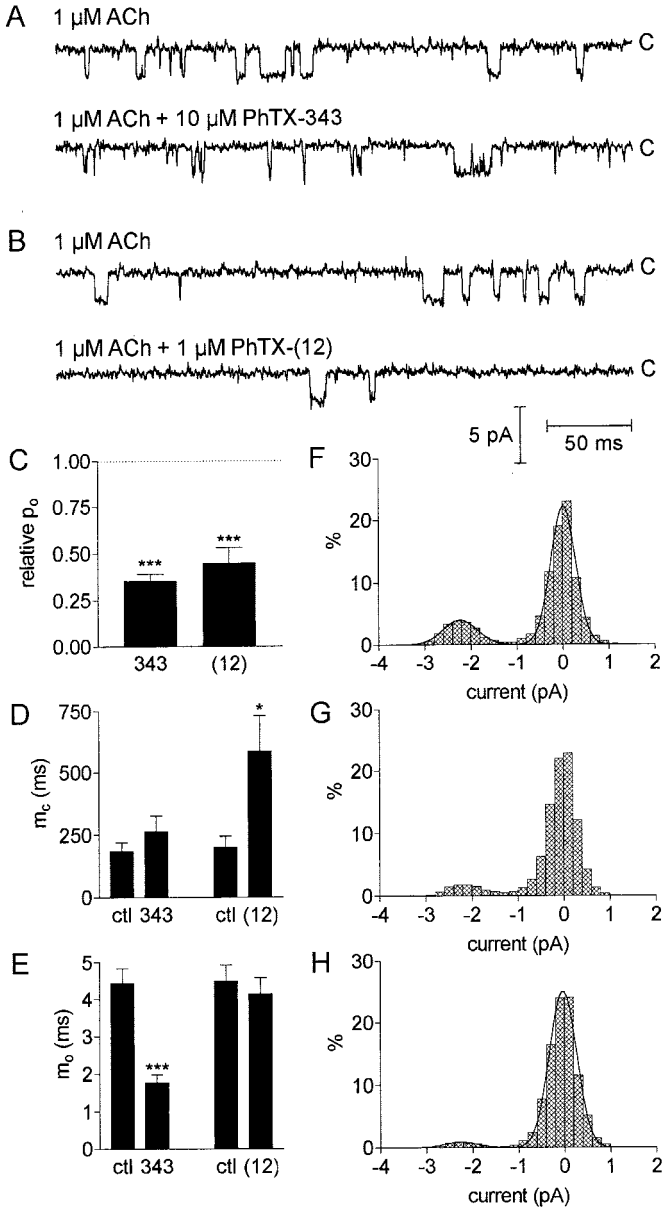

Fig. 9. Effect of PhTX-343 and PhTX-(12) on single-channel parameters in outside-out patches. A and B, single-channel recordings in response to 1 μM ACh in the absence (top trace) and presence (bottom trace) of either 10 μM PhTX-343 (A) or 1 μM PhTX-(12) (B). C–E, bar graphs showing open probability (P_o) relative to controls (C), m_c (D), and m_o (E) for single-channel events in the absence (ctl) and presence of either 10 μM PhTX-343 or 1 μM PhTX-(12). Significant differences from control values are indicated by * ($P < 0.05$) or *** ($P < 0.001$). F–H, all-points histograms of single-channel data (from the same patch) evoked by 1 μM ACh alone (F) or in the presence of either 10 μM PhTX-343 (G) or 1 μM PhTX-(12) (H). The histograms in F and H are fit by the sum of two Gaussian distributions with peak separations of 2.24 pA (F) and 2.21 pA (H), corresponding to conductances of 37.3 and 36.8 pS, respectively. V_H was −60 mV in all cases.

current inhibition was consistently greater than peak current inhibition. The fact that PhTX-(12) antagonism is weakly voltage-dependent whereas antagonism by PhTX-343 is strongly voltage-dependent leads us to conclude that these philanthotoxins share two binding sites on nAChR: one deep within the membrane electric field, for which PhTX-343 has a preference, and one at a more extracellular position, for which PhTX-(12) has a dominant preference. It follows that the main action of PhTX-(12) is on the closed-channel conformation of nAChR, whereas that of PhTX-343 is on the open- and closed-channel conformations. Because inhibition by PhTX-(12) is accompanied by an increase in the rate of decay of the response to ACh, requires receptor activation, and is enhanced when PhTX-(12) is preapplied, we further conclude that when PhTX-(12) and PhTX-343 bind to the closed channel conformation of nAChR of TE671 cells, they enhance desensitization.

The weak voltage dependence of antagonism and the stronger voltage dependence of recovery from antagonism by PhTX-(12) suggest a binding site for this toxin at the external mouth of the pore that may extend into the channel vestibule. Such a site has been photoaffinity-labeled by the aromatic region of the closely related compound ^{125}I-MR44 (Bixel et al., 2001). MR44 antagonizes nAChR in a manner identical to that of PhTX-(12) [i.e., weakly voltage-dependent inhibition that is activation-dependent (Brier et al., 2002)]. Significantly, Matsushima et al. (2002) have shown that mutation of Ser-284 to Leu or Phe in the α4-subunit results in a faster desensitization rate. This residue is conserved in the human α1 subunit (Ser- 297). Perhaps the terminal amine group of PhTX-(12) (and of MR44) interacts with this residue to "neutralize" it in the same way as mutation to a hydrophobic residue. It seems clear that hydrophilic philanthotoxin analogs (e.g., PhTX-343) with multiple amino groups can bind at site deep in the ion channel pore, whereas hydrophobic analogs [e.g., PhTX-(12)] act at a shallower site in the pore to enhance desensitization.

References

Anis N, Sherby S, Goodnow R, Niwa M, Konno K, Kallimopoulos T, Bukownik R, Nakanishi K, Usherwood PNR, Eldefrawi A, et al. (1990) Structure-activity-relationships of philanthotoxin analogues and polyamines on *N*-methyl-D-aspartate and nicotinic acetylcholine receptors. *J Pharmacol Exp Ther* **254:**764–773.

Arias HR (1998) Binding sites for exogenous and endogenous non-competitive inhibitors of the nicotinic acetylcholine receptor. *Biochim Biophys Acta* **1376:**173–220.

Bähring R and Mayer ML (1998) An analysis of philanthotoxin block for recombinant rat GluR6(Q) glutamate receptor channels. *J Physiol* **509:**635–650.

Benson JA, Schürmann F, Kaufmann L, Gsell L, and Piek T (1992) Inhibition of dipteran larval neuromuscular synaptic transmission by analogues of philanthotoxin-4.3.3: a structure-activity study. *Comp Biochem Physiol C* **102:**267–272.

Benson JA, Kaufmann L, Hue B, Pelhate M, Schürmann F, Gsell L, and Piek T (1993) The physiological action of analogues of philanthotoxin-4.3.3 at insect nicotinic acetylcholine receptors. *Comp Biochem Physiol C* **105:**303–310.

Bixel MG, Krauss M, Liu Y, Bolognesi ML, Rosini M, Mellor IR, Usherwood PNR, Melchiorre C, Nakanishi K, and Hucho F (2000) Structure-activity relationship and site of binding of polyamine derivatives at the nicotinic acetylcholine receptor. *Eur J Biochem* **267:**110–120.

Bixel GM, Weise C, Bolognesi ML, Rosini M, Brierly MJ, Mellor IR, Usherwood PNR, Melchiorre C, and Hucho F (2001) Location of the polyamine binding site in the vestibule of the nicotinic acetylcholine receptor ion channel. *J Biol Chem* **276:**6151–6160.

Blagbrough IS and Usherwood PNR (1992) Polyamine amide toxins as pharmacological tools and pharmaceutical agents. *Proc R Soc Edinb Sect B (Biol Sci)* **99:**67–81.

Brackley PTH, Bell DR, Choi SK, Nakanishi K, and Usherwood PNR (1993) Selective antagonism of native and cloned kainate and NMDA receptors by polyamine containing toxins. *J Pharmacol Exp Ther* **266:**1573–1580.

Brier TJ, Mellor IR, and Usherwood PNR (2002) Allosteric and steric interactions of polyamines and polyamine-containing toxins with nicotinic acetylcholine receptors, in *Perspectives in Molecular Toxinology* (Ménez A ed) pp 281–297, John Wiley and Sons Ltd, Chichester, UK.

Bruce M, Bukownik R, Eldefrawi AT, Eldefrawi ME, Goodnow R, Kallimopoulos T, Konno K, Nakanishi K, Niwa M, and Usherwood PNR (1990) Structure activity relationships of analogues of the wasp toxin philanthotoxin: noncompetitive antagonists of quisqualate receptors. *Toxicon* **28:**1333–1346.

Charnet P, Labarca C, Leonard RJ, Vogelaar NJ, Czyzyk L, Gouin A, Davidson N, and Lester HA (1990) An open-channel blocker interacts with adjacent turns of α-helices in the nicotinic acetylcholine receptor. *Neuron* **2:**87–95.

Corringer P-J, Le Novère N, and Changeux J-P (2000) Nicotinic receptors at the amino acid level. *Annu Rev Pharmacol Toxicol* **40:**431–458.

Eldefrawi AT, Eldefrawi MF, Konno K, Mansour NA, Nakanishi K, Oltz E, and Usherwood PNR (1988) Structure and synthesis of a potent glutamate receptor antagonist in wasp venom. *Proc Natl Acad Sci USA* **85:**4910–4913.

Giraudat J, Dennis M, Heidmann T, Chang JY, and Changeux JP (1986) Structure of the high affinity binding site for non-competitive blockers of the acetylcholine receptor: Serine 262 of the δ-subunit is labeled by [^{3}H]chlorpromazine. *Proc Natl Acad Sci USA* **83:**2719–2723.

Itier V and Bertrand D (2001) Neuronal nicotinic receptors: from protein structure to function. *FEBS Lett* **504:**118–125.

Jackson H and Usherwood PNR (1988) Spider toxins as tools for dissecting elements of excitatory amino acid transmission. *Trends Neurosci* **11:**278–283.

Jaroszewski JW, Matzen L, Frølund B, and Krogsgaard-Larsen P (1996) Neuroactive polyamine wasp toxins: Nuclear magnetic resonance spectroscopic analysis of the protolytic properties of philanthotoxin-343. *J Med Chem* **39:**515–521.

Jayaraman V, Usherwood PNR, and Hess GP (1999) Inhibition of nicotinic acetylcholine receptor by philanthotoxin-343: kinetic investigations in the microsecond time region using a laser-pulse photolysis technique. *Biochem* **38:**11406–11414.

Jones GM, Anis NA, and Lodge D (1990) Philanthotoxin blocks quisqualate-, AMPA- and kainate-, but not NMDA-, induced excitation of rat brainstem neurones in vivo. *Br J Pharmacol* **101:**969–970.

Karst H, Piek T, Van Marle J, Lind A, and Van Weeren-Kramer J (1991) Structure-activity relationship of philanthotoxins-I. Pre- and postsynaptic inhibition of the locust neuromuscular transmission. *Comp Biochem Physiol* **98C:**471–477.

Karst H and Piek T (1991) Structure-activity relationship of philanthotoxins-II. Effects on the glutamate gated ion channels of the locust muscle fibre membrane. *Comp Biochem Physiol* **98C:**479–489.

Liu M, Nakazawa K, Inoue K, and Ohno Y (1997) Potent and voltage-dependent block by philanthotoxin-343 of neuronal nicotinic receptor/channels in PC12 cells. *Br J Pharmacol* **122:**379–385.

Lukas RJ, Changeux JP, Le Novere N, Albuquerque EX, Balfour DJ, Berg DK, Bertrand D, Chiappinelli VA, Clarke PB, Collins AC, et al. (1999) International Union of Pharmacology. XX. Current status of the nomenclature for nicotinic acetylcholine receptors and their subunits. *Pharmacol Rev* **51:**397–401.

Matsushima N, Shinichi H, Iwata H, Fukuma G, Yonetani M, Nagayama C, Hamanaka W, Matsunaka Y, Ito M, Kaneko S, et al. (2002) Mutation (Ser284Leu) of neuronal nicotinic acetylcholine receptor α4 subunit associated with frontal lobe epilepsy causes faster desensitization of the rat receptor expressed in oocytes. *Epilepsy Res* **48:**181–186.

Mellor IR, Brier TJ, Pluteanu F, Strømgaard K, Saghyan A, Eldursi N, Brierley MJ, Andersen K, Jaroszewski JW, Krogsgaard-Larsen P and Usherwood PNR (2003) Modification of the philanthotoxin-343 polyamine moiety results in different structure-activity profiles at muscle nicotinic ACh, NMDA and AMPA receptors. *Neuropharmacol* **44:**70–80.

Nakanishi K, Huang X, Jiang H, Liu Y, Fang K, Huang D, Choi SK, Katz E, and Eldefrawi M (1997) Structure-binding relation of philanthotoxins from nicotinic acetylcholine receptor binding assay. *Bioorg Med Chem* **5:**1969–1988.

Oswald RE, Papke RI, and Lukas RJ (1989) Characterization of nicotinic acetylcholine receptor channels of the TE671 human medulloblastoma clonal line. *Neurosci Lett* **96:**207–212.

Piek T and Hue B (1989) Philanthotoxins, a new class of neuroactive polyamines, block nicotinic transmission in the insect CNS. *Comp Biochem Physiol C Pharmacol Toxicol Endocrinol* **93:**403–406.

Ragsdale D, Gant DB, Anis NA, Eldefrawi AT, Eldefrawi ME, Konno K, and Miledi R (1989) Inhibition of rat brain glutamate receptors by philanthotoxin. *J Pharmacol Exp Ther* **251:**156–163.

Rozental R, Scoble GT, Albuquerque EX, Idriss M, Sherby S, Sattelle DB, Nakanishi K, Konno K, Eldefrawi AT, and Eldefrawi ME (1989) Allosteric inhibition of nicotinic acetylcholine receptors of vertebrates and insects by philanthotoxin. *J Pharmacol Exp Ther* **249:**123–130.

Schoepfer R, Luther M, and Lindstrom J (1988) The human medulloblastoma cell line TE671 expresses a muscle like acetylcholine receptor - cloning of the α-subunit cDNA. *FEBS Lett* **226:**235–240.

Shao Z, Mellor IR, Brierley MJ, Harris J, and Usherwood PNR (1998) Potentiation and inhibition by spermine of nicotinic acetylcholine receptors in the TE671 human muscle cell line. *J Pharmacol Exp Ther* **286:**1269–1276.

Strømgaard K, Brierley MJ, Andersen K, Sløk FA, Mellor IR, Usherwood PNR, Krogsgaard-Larsen P and Jaroszewski JW (1999) Analogues of neuroactive polyamine wasp toxins that lack inner basic sites exhibit enhanced antagonism towards a muscle-type mammalian nicotinic acetylcholine receptor. *J Med Chem* **42:**5224–5234.

Strømgaard K, Brier TJ, Andersen K, Mellor IR, Usherwood PNR, Krogsgaard-Larsen P, and Jaroszewski JW (2000) Synthesis and biological eveluation of a combinatorial library of philanthotoxin analogues. *J Med Chem* **43:**4526–4533.

Strømgaard K, Mellor IR, Andersen K, Neagoe I, Pluteanu F, Usherwood PNR, Krogsgaard-Larsen P, Jaroszewski JW (2002) Solid-phase synthesis and pharmacological evaluation of analogues of PhTX-12 - a potent and selective nicotinic acetylcholine receptor antagonist. *Bioorg Med Chem Lett* **12:**1159–1162.

Tikhonov DB, Magazanik LG, Mellor IR, and Usherwood PNR (2000) Possible influence of intramolecular hydrogen bonds on the three-dimensional structure of polyamine amides and their interaction with ionotropic glutamate receptors. *Recept Channels* **7:**227–236.

Usherwood PNR and Blagbrough IS (1991) Spider toxins affecting glutamate receptors: polyamines in therapeutic neurochemistry. *Pharmacol Ther* **52:**245–268.

Wellendorph P, Jaroszewski JW, Hansen SH, and Franzyk H (2003) A sequential high-yielding large-scale solution-method for synthesis of philanthotoxin analogues. *Eur J Med Chem* **38:**117–122.

Woodhull AM (1973) Ionic blockage of sodium channels in nerve. *J Gen Physiol* **61:**687–708.

Address correspondence to: Dr. Ian R. Mellor, School of Life and Environmental Sciences, University of Nottingham, University Park, Nottingham, NG7 2RD, UK. E-mail: ian.mellor@nottingham.ac.uk